First-principles investigations of transition metal dihydrides, TH_2: T = Sc, Ti, V, Y, Zr, Nb; energetics and chemical bonding

2000 J. Phys.: Condens. Matter 12 4535

(http://iopscience.iop.org/0953-8984/12/21/301)

J. Phys.: Condens. Matter **12** (2000) 4535–4551. Printed in the UK PII: S0953-8984(00)10994-4

First-principles investigations of transition metal dihydrides, TH_2: T = Sc, Ti, V, Y, Zr, Nb; energetics and chemical bonding

Walter Wolf† and Peter Herzig

Institut für Physikalische Chemie, Universität Wien, Währinger Straße 42, A-1090 Vienna, Austria

Received 13 January 2000, in final form 10 April 2000

Abstract. Self-consistent full-potential linearized augmented-plane-wave (LAPW) band-structure calculations are performed for the fluorite-type dihydrides ScH_2, TiH_2, VH_2, YH_2, ZrH_2 and NbH_2 as well as for the tetragonal low-temperature phases of TiH_2 and ZrH_2. For all compounds studied which show metallic behaviour, band structures, densities of states, electron densities and the total-energy minima with respect to the lattice parameters are computed. Additionally, the bulk moduli for the cubic phases are given. Good agreement with experimental data is found where they are available. The results obtained confirm previous interpretations of the tetragonal distortion of the cubic unit cell as a Jahn–Teller-type effect and show how the electron densities of the tetragonally distorted phases depend on the splitting of states near the Fermi level. The total-energy curves for TiH_2 and ZrH_2 as functions of the c/a ratios show two minima each, of which only the ones for $c/a < 1$ have been observed experimentally.

1. Introduction

Many transition metals (as well as rare-earth metals) react readily with hydrogen to form hydrides (see, e.g., Fukai 1993). In the present paper the dihydrides of the transition elements from the groups 3–5 of the periodic table are investigated systematically as regards their equilibrium lattice parameters and their electronic and chemical bonding properties. These dihydrides either have the cubic fluorite structure or, in the case of the dihydrides formed from group 4 transition metals, a tetragonally distorted fluorite structure.

The amount of structural information and the details of the phase diagrams are dependent on the transition metal. While the yttrium–hydrogen system has attracted much attention recently due to the still open question of what causes the experimentally found band gap near the composition YH_3 (Kelly *et al* 1997, Ng *et al* 1997, Hjörvarsson *et al* 1999), hydrides of such composition have not been found for Sc. The dihydrides YH_2 (Daou and Vajda 1992) and ScH_2 (Khodyrev and Baranova 1980) both have CaF_2 structure. The dihydrides TiH_2 and ZrH_2 have a tetragonally distorted fluorite structure (Ducastelle *et al* 1970). The phase diagram of the Zr–H system can be found in Zuzek *et al* (1990). For TiH_2 there is a second-order phase transition to the cubic phase at about 300 K while the tetragonal phase of ZrH_2 is stable to much higher temperatures (Yakel 1958, Ducastelle *et al* 1970). This phase transition between the cubic and the tetragonal phase has been suggested by Ducastelle *et al* (1970) to be of Jahn–Teller type. The phase diagrams for vanadium–hydrogen and niobium–hydrogen systems have been given by Reilly and Wiswall (1970) for compositions between the pure metal and the dihydride.

† Present address: Molecular Simulations, Parc Club Orsay Université, 20, rue Jean Rostand, F-91893 Orsay Cédex, France.

0953-8984/00/214535+17$30.00

Investigations of the electronic structures of stoichiometric and substoichiometric transition metal dihydrides by means of transition metal and proton NMR measurements have been performed by, among others, Nowak *et al* (1979, 1982), Żogał and Idziak (1981), Nowak and Minier (1984), Niedźwiedź *et al* (1993) and Żogał *et al* (1999). A theoretical analysis of the nuclear spin–lattice relaxation rates for ScH_2, TiH_2, VH_2 and NbH_2 based on LAPW band-structure calculations has led to good agreement for the first two and to only fair agreement for the latter two dihydrides (Żogał *et al* 1996).

Previous band-structure calculations for the dihydrides treated in the present paper have been numerous since Switendick's (1970) first and pioneering paper in this field (for a review see Gupta and Schlapbach 1988). In addition to Er and Pr di- and trihydrides he investigated YH_2 and YH_3 using the non-self-consistent augmented-plane-wave (APW) method. Employing the same method he later performed calculations for cubic and tetragonal TiH_2 and ZrH_2 (Switendick 1976, 1984) in order to study the phase transition in these two systems. The electronic structure of TiH_2, ZrH_2 and NbH_2 (with particular attention to the Jahn–Teller effect in the first two compounds) has also been studied by Gupta (1979, 1982) on the basis of the non-self-consistent APW method. Other band-structure investigations relevant and important in the present context are the non-self-consistent APW investigation of TiH_2 by Fujimori and Tsuda (1982), self-consistent APW calculations for the titanium and zirconium (and hafnium) dihydrides by Papaconstantopoulos and Switendick (1984) and the subsequent paper by Papaconstantopoulos *et al* (1986) where the authors use the previously obtained APW results to perform tight-binding coherent-potential-approximation (TB-CPA) calculations for cubic $TiH_{1.6}$ and $VH_{1.6}$ (assuming statistically distributed H vacancies) in order to draw conclusions as regards the stability of the substoichiometric cubic Ti and V dihydrides. The Korringa–Kohn–Rostoker (KKR) method was used in a non-self-consistent fashion by Kulikov and Zvonkov (1979) and self-consistently by Peterman and Harmon (1979) as well as by Peterman *et al* (1979a, b) for ScH_2 and YH_2. The electronic structure of VH_2 and NbH_2 has been calculated by Sen Gupta and Chatterjee (1982) using a variant of the APW method. On the basis of total-energy calculations made using a mixed-basis set pseudopotential approach, Elsässer *et al* (1997) studied the optic vibrational modes of TiH_2 and ZrH_2 and compared the calculated excitation energies with experimental results obtained by means of inelastic neutron scattering. Very recently, Matumura *et al* (1999) employed the DV X_α cluster method to study alloying effects on the electronic structures of VH_2 and V_2H.

An attempt to achieve a deeper theoretical understanding of the hydride formation of zirconium has been made lately by Ackland (1998a). Arguing on the basis of a process called delayed hydride cracking (DHC; Smith (1995) and references therein), Ackland calculates the energy surface for the tetragonal ϵ-phase as a function of the lattice parameters a and c using a pseudopotential method. He obtains a double minimum in the energy surface, one minimum for $c/a < 1$ and the other for $c/a > 1$ with an energy barrier in between of roughly 0.1 eV. (The energy minimum for $c/a < 1$ is found at a- and c-values very close to the experimental values for the macroscopic tetragonal ϵ-phase.) This double-minimum structure implies that a small stress will lead to a transition between the two structures accompanied by a large strain, a behaviour which plays an important role in understanding the δ–ϵ phase transition for ZrH_2. Unfortunately, Ackland's density-of-states (DOS) curves are obviously in error (Gupta 1998, Ackland 1998b), but he claims that the other results are not affected.

Further total-energy calculations for the dihydrides have until now only been performed in connection with the hydrogen ordering of hydride phases containing more than two hydrogen atoms per transition or rare-earth metal (Sun *et al* 1994, Wang and Chou 1994, 1995). The structures of these hydrides can be thought to be derived from the fluorite structure by filling additional H atoms into the octahedral sites of the structure. The ordering of the hydrogen

atoms at the octahedral sites is not yet fully understood. An interesting feature in these systems is the contraction of the lattice with increasing hydrogen content (Wang and Chou 1994). In a forthcoming paper (Herzig *et al* 1999) the calculated electric field gradients for deuterium in ordered YD_3 and several hypothetical ordered structures for $YD_{2.25}$ are calculated and compared to experimental results.

The aim of the present work is to investigate the electronic structures of the six dihydrides ScH_2, TiH_2, VH_2, YH_2, ZrH_2 and NbH_2 with consistent accuracy on the basis of the density functional theory. Band structures, DOS, local partial DOS and, for the first time, valence electron densities are presented and used to discuss the chemical bonding in these compounds. Total-energy calculations are used to calculate the equilibrium lattice parameters both for the cubic and for the tetragonal phases as well as their relative stability in terms of differences in total energy. From the volume dependence of the total energies the bulk moduli of the cubic phases are evaluated.

2. Computational details

For the electronic band-structure calculations the full-potential linearized augmented-plane-wave (FLAPW) method (see, for instance, Wimmer *et al* 1981, Jansen and Freeman 1984) with an exchange–correlation potential given by Hedin and Lundqvist (1971, 1972) was used. For the l-expansion of the potential and the electron density within the muffin-tin spheres, terms up to $l = 8$ were taken into account. For the wave function, plane waves in the interstitial region were included up to a length of $5\frac{2\pi}{a}$. The chosen plane-wave basis corresponds to approximately 300–600 basis functions. The self-consistency procedure has been performed with 252 $\boldsymbol{k}$-points in the irreducible part of the Brillouin zone (IBZ) of the fcc Bravais lattice (for the fluorite structure, space group $Fm\bar{3}m$, No 225) and with 395 $\boldsymbol{k}$-points for the IBZ of the body-centred-tetragonal lattice (for the tetragonally distorted fluorite structure, space group $I4/mmm$, No 139). The same mesh of $\boldsymbol{k}$-points has also been used for the calculation of the electron density and DOS plots. The Brillouin-zone integration was performed by means of the linear tetrahedron method (Jepsen and Andersen 1971, Lehmann and Taut 1972). The bulk moduli have been obtained using a so-called Birch fit for the total energy as a function of the volume (Birch 1938, 1952, 1978).

The muffin-tin radii used in the FLAPW band-structure calculation are given in table 1. They have been kept constant for all lattice geometries.

Table 1. Muffin-tin radii (in au) used in the FLAPW band-structure calculations.

Compound	R_T	R_H
ScH_2	2.24981	1.43460
TiH_2	2.09280	1.33448
VH_2	1.95500	1.33448
YH_2	2.65080	1.33448
ZrH_2	2.34400	1.33448
NbH_2	2.18056	1.33448

3. Results and discussion

3.1. Cubic phases

3.1.1. Equilibrium lattice parameters and bulk moduli. In table 2 the calculated equilibrium lattice parameters are compared to typical experimental results. The agreement is very

Table 2. Calculated equilibrium lattice parameters (this work) and experimental values (in Å) for the cubic dihydrides.

Compound	a_{calc}	a_{exp}	Remarks	References
ScH_2	4.7409	4.78		Khodyrev and Baranova (1980)
TiH_2	4.3986	4.460	$TiH_{1.95}$	Ducastelle *et al* (1970)
VH_2	4.1873	4.271		Müller and Weymann (1986)
YH_2	5.2001	5.2032	90 K	Daou and Vajda (1992)
ZrH_2	4.8040	4.780	$ZrH_{1.55}$	Ducastelle *et al* (1970)
NbH_2	4.5518	4.566		Müller and Weymann (1986)

satisfactory, if one bears in mind the tendency towards overbinding in the local density approximation (LDA) of the density functional theory, which leads to calculated lattice parameters that are normally about 1–2% too small. Consistent with experience, also for the hydrides the LDA overbinding effect is more pronounced for compounds of 3d transition metals than for 4d or 5d transition metal compounds. (A larger lattice parameter a is obtained for ZrH_2, because the experimental value refers to the composition $ZrH_{1.55}$ of the cubic δ-phase.) A previous result obtained by Switendick (1987) for TiH_2 also agrees well with the present one. All results given in the remainder of this paper are based on the theoretical equilibrium lattice parameters.

Using Birch fits for the total energy as a function of the lattice parameters, the bulk moduli are obtained. They are shown in table 3. No experimental values for comparison seem to be available in the literature so far. It is anticipated that experimentally measured bulk moduli might be somewhat smaller than the calculated ones due to LDA overbinding (about 5–10% for 3d compounds). For hydrides of transition metals of the same period the usual trend of increasing bulk moduli with decreasing lattice parameters is observed. For hydrides of metals within the same column of the periodic table, the bulk moduli are very close to each other despite large differences in the lattice parameters.

Table 3. Calculated bulk moduli (in GPa) for the cubic dihydrides.

ScH_2	TiH_2	VH_2
109.2	162.0	200.4
YH_2	ZrH_2	NbH_2
101.1	151.6	197.5

3.1.2. Band structures and DOS. The band structures for the valence bands of the six cubic dihydrides investigated in this paper are shown in figure 1. Two of the seven lowest bands shown originate from the 1s states of the two hydrogen atoms per unit cell and the other five bands from the Ti 3d states. The lowest of the bands shown has a relatively pronounced hydrogen s character that corresponds to bonding H–H s–s σ-interactions, as can be seen below from the local partial H s DOS (figure 2) and from some electron density plots for single electronic states for TiH_2 (figure 5). There is also a band (above the Fermi level) that corresponds to antibonding H–H s–s σ^*-interactions.

It can be clearly seen from figure 1 that the rigid-band model is fulfilled to a good degree, which means that the band structures are only changed slightly from ScH_2 to VH_2 and from YH_2 to NbH_2 apart, of course, from the shift of the Fermi level towards higher energies due to the two additional valence electrons.

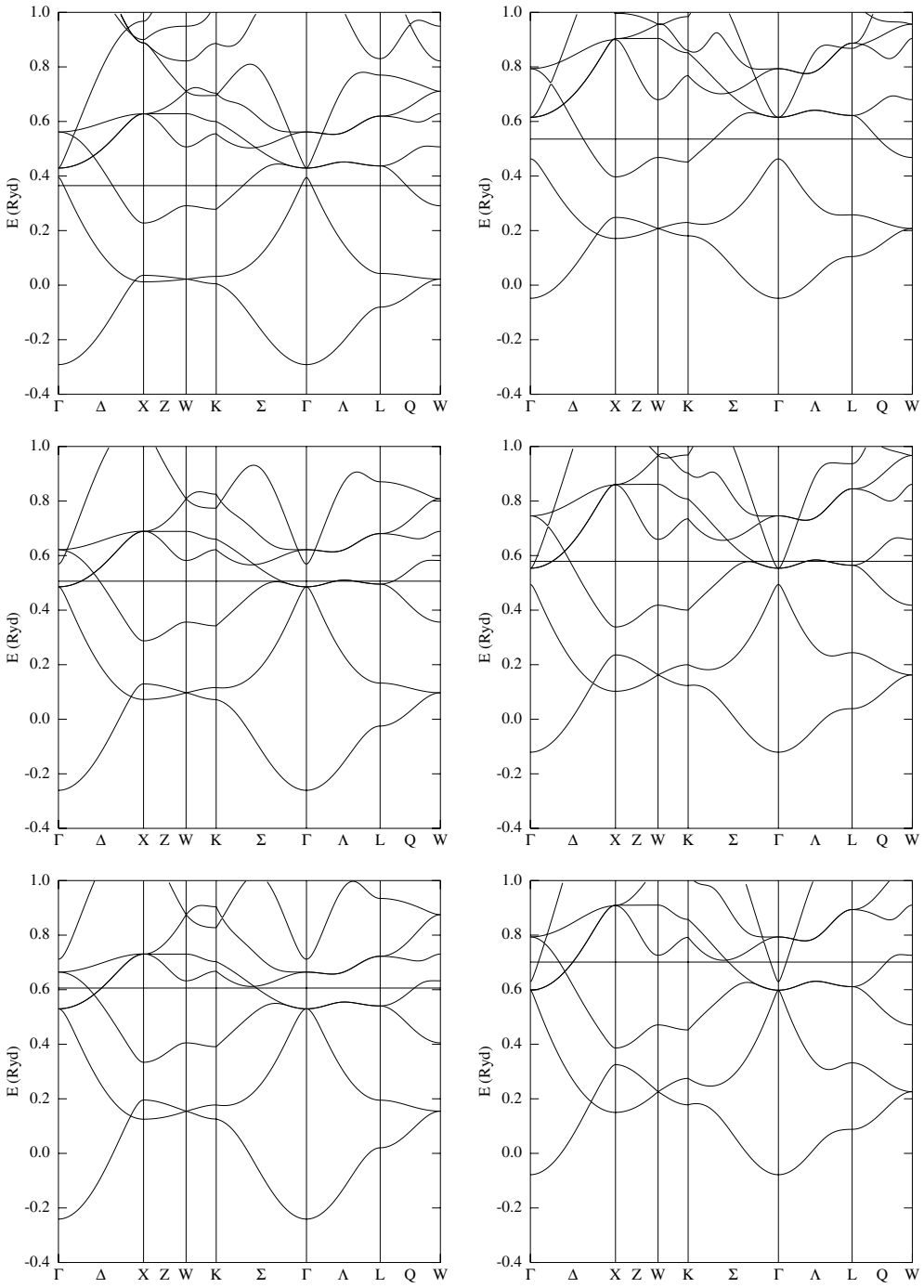

Figure 1. Band structures of fluorite-type ScH_2 (top left), TiH_2 (centre left), VH_2 (bottom left), YH_2 (top right), ZrH_2 (centre right) and NbH_2 (bottom right). The energy scale is with respect to the averaged potential in the interstitial region.

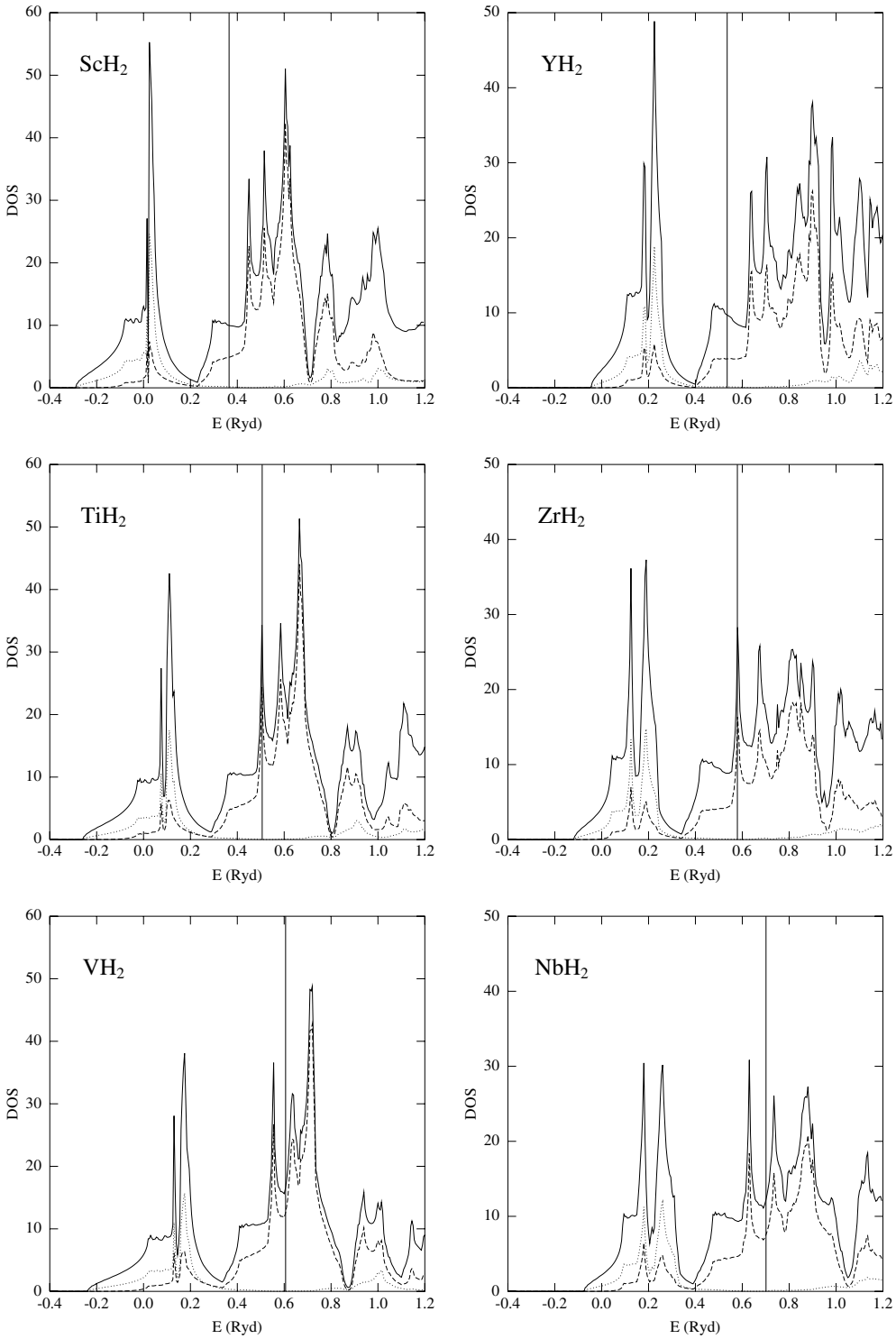

Figure 2. The total DOS (full line), and H s (dotted line) and transition metal d (dashed line) local partial DOS components for fluorite-type ScH_2, TiH_2, VH_2, YH_2, ZrH_2 and NbH_2 in units of one-electron states per Rydberg and per unit cell.

Figure 2 shows the total DOS and the most important l-like components, i.e., H s and transition metal d. At the low-energy side of the DOS only H s contributions are found for all hydrides discussed here. (Notice that the discrepancy between the total and H s-like DOS comes from the interstitial region where a classification in terms of l is not performed.) There then follows an energy region (until the deep minimum in the DOS is reached) where both H s and transition metal d components are present. It corresponds to states that form Ti–H d–s σ-bonds and also Ti–Ti d–d σ-bonds. From the deep DOS minimum to the Fermi level, H s states contribute very little to the total DOS. In this energy range Ti d states dominate by far. They have mainly e_g character where the DOS curve is almost horizontal and t_{2g} character at the position of the sharp peak that is above the Fermi level for ScH_2 and YH_2, at the Fermi level for TiH_2 and ZrH_2 and below the Fermi level for VH_2 and NbH_2. (This can, e.g., be seen from the density plots in the bottom part of figure 5—see later.) The fact that the Fermi energy coincides with the position of the sharp peaks for TiH_2 and ZrH_2 suggests that the cubic phases are not stable at low temperatures. It will be shown below that the tetragonal Jahn–Teller distortion leads to split of this peak into two with a minimum at the Fermi energy which leads to a lowering of the total energy.

3.1.3. Electron densities and chemical bonding. Figures 3 and 4 present the valence electron densities in the (100) plane (through the transition metal atoms) and in the (110) plane, respectively. The appearance of the density plots depends considerably on the number of valence electrons. For the group 3 dihydrides the spherical shape of the contour lines between the transition metal atoms is caused by the H atoms above and below the plane of the drawing (figure 3). Also the fact that the H atoms look much bigger for ScH_2 or for YH_2 than for VH_2 or for NbH_2 is, at least to some extent, caused by the higher number of valence electrons in the group 5 dihydrides (figure 4). From both figures it can be seen that the proportion of e_g character in the density about the metal atoms is decreasing with the increase of the number of valence electrons. This is due to the fact that the sharp peak near the Fermi level, which is fully occupied only for VH_2 and NbH_2, has predominantly t_{2g} character.

The main bonding types in the dihydrides are illustrated in figure 5 by the electron density plots for some single states for TiH_2. The two plots in the upper row show H–H s–s σ-bonds and Ti–H d–s σ-bonds and in the lower row Ti–Ti t_{2g}–t_{2g} and e_g–e_g σ-bonds. Other bonding types of minor importance can, of course, be identified, e.g., Ti–Ti t_{2g}–t_{2g} π-interactions (between second-nearest Ti neighbours) and Ti–Ti e_g–e_g π-interactions (between nearest Ti neighbours).

3.2. Tetragonal phases

3.2.1. Total energies. The total-energy curves for TiH_2 and ZrH_2 as functions of the c/a ratios are given in figure 6. They both show the same double-minimum structure as previously found by Ackland (1998a) for ZrH_2. Good agreement with his results and also with the experimental results for the minima for $c/a < 1$ for both hydrides is obtained (table 4). There is, however, a small discrepancy between Ackland's and this work. While Ackland obtains a deeper minimum for $c/a > 1$, in our calculation the opposite is true. Since the difference is only a few tenths of a millirydberg it is not clear whether this is physically relevant. For TiH_2 we obtain a slightly deeper minimum for $c/a > 1$.

It should be noted here that the very small energy differences observed for these transitions make a decisive statement difficult. Although our calculations can be considered as well converged with respect to computational parameters, some more fundamental approximations have to be taken into account. The present investigation is based on the density functional

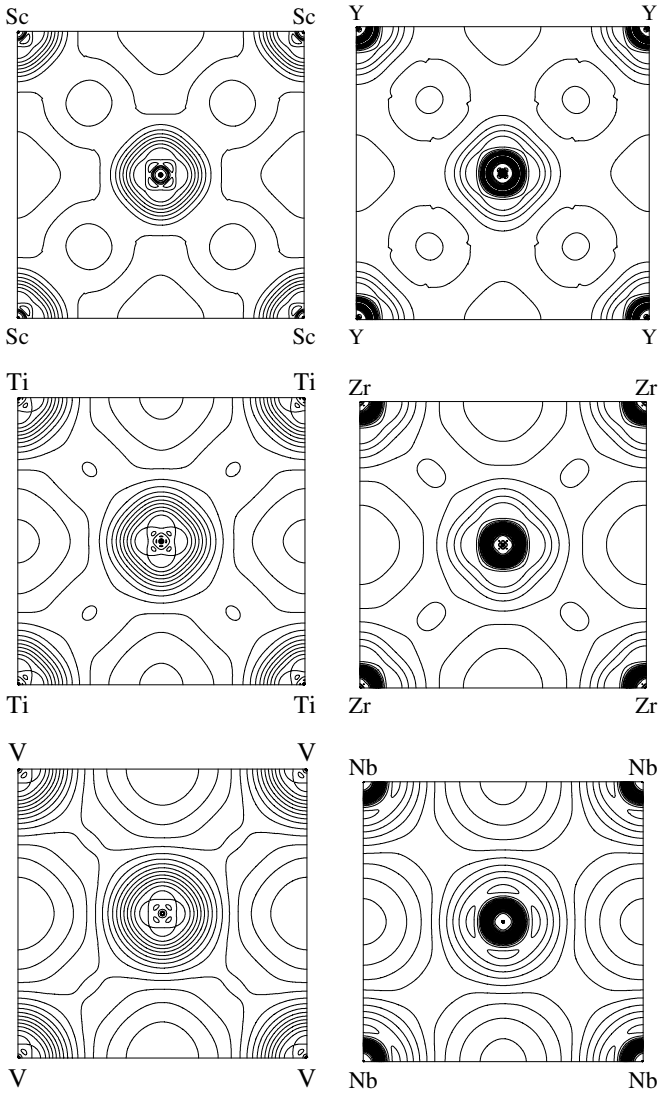

Figure 3. Valence electron densities in the (100) plane for fluorite-type ScH_2 (top left), TiH_2 (centre left), VH_2 (bottom left), YH_2 (top right), ZrH_2 (centre right) and NbH_2 (bottom right). A logarithmic grid of contour lines has been used ($x_i = x_0 2^{i/3}$, $x_0 = 0.2\ e\ \text{Å}^{-3}$).

theory applied in the local density approximation. It has been shown by Ackland (1998a) that the more sophisticated generalized gradient approximation (Perdew and Wang 1992) does not change the energetics in this case. Furthermore, the contribution of zero-point vibrations of the hydrogen atoms might be different for the cubic and tetragonally distorted structures. Zero-point vibrations were included in a recent study of cubic TiH_2 and ZrH_2 by Elsässer *et al* (1997), but were not taken into account for the present study.

3.2.2. Band structures and DOS. In figure 7 the band structures for cubic TiH_2 and ZrH_2 are compared to the band structures for the two different tetragonal distortions. For both cubic compounds there is a band going from the Γ to the L point in the face-centred cubic Brillouin

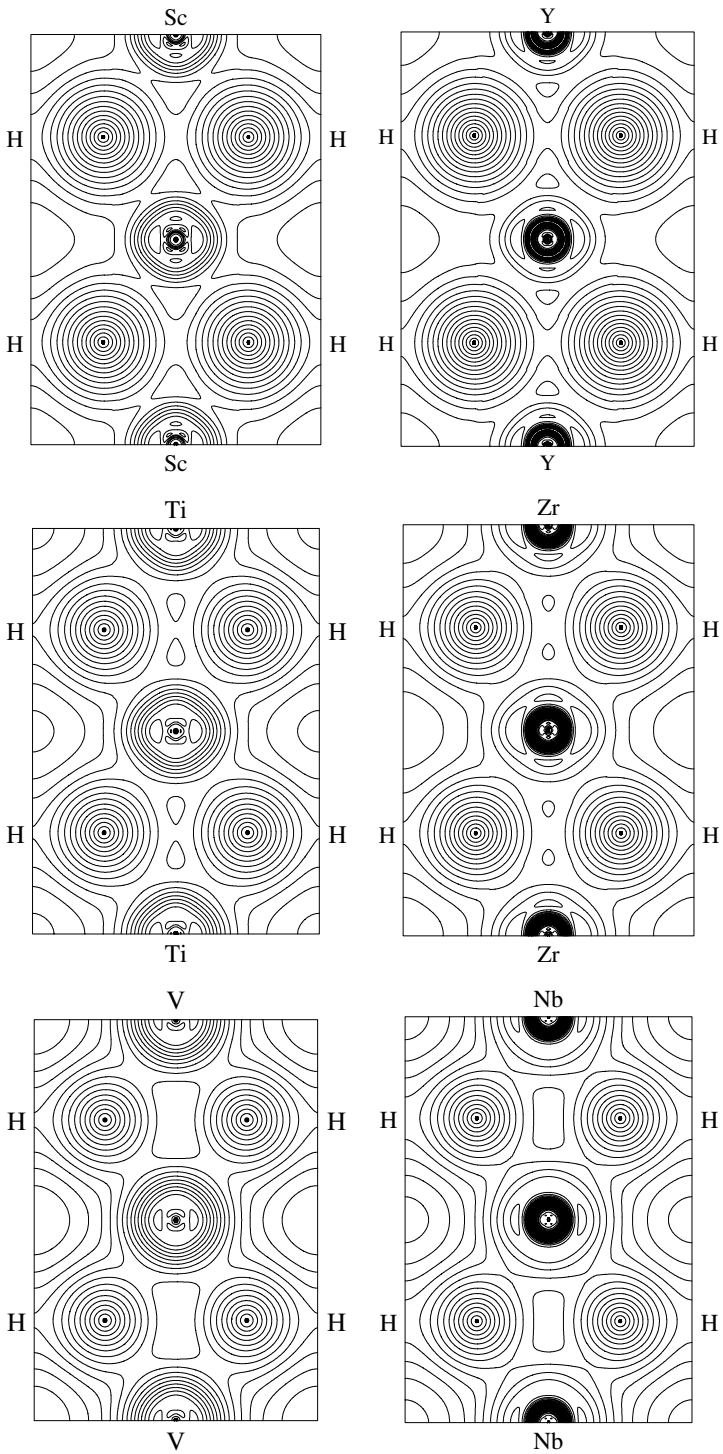

Figure 4. Valence electron densities in the (110) plane for fluorite-type ScH_2 (top left), TiH_2 (centre left), VH_2 (bottom left), YH_2 (top right), ZrH_2 (centre right) and NbH_2 (bottom right). A logarithmic grid of contour lines has been used ($x_i = x_0 2^{i/3}$, $x_0 = 0.2\ e$ Å^{-3}).

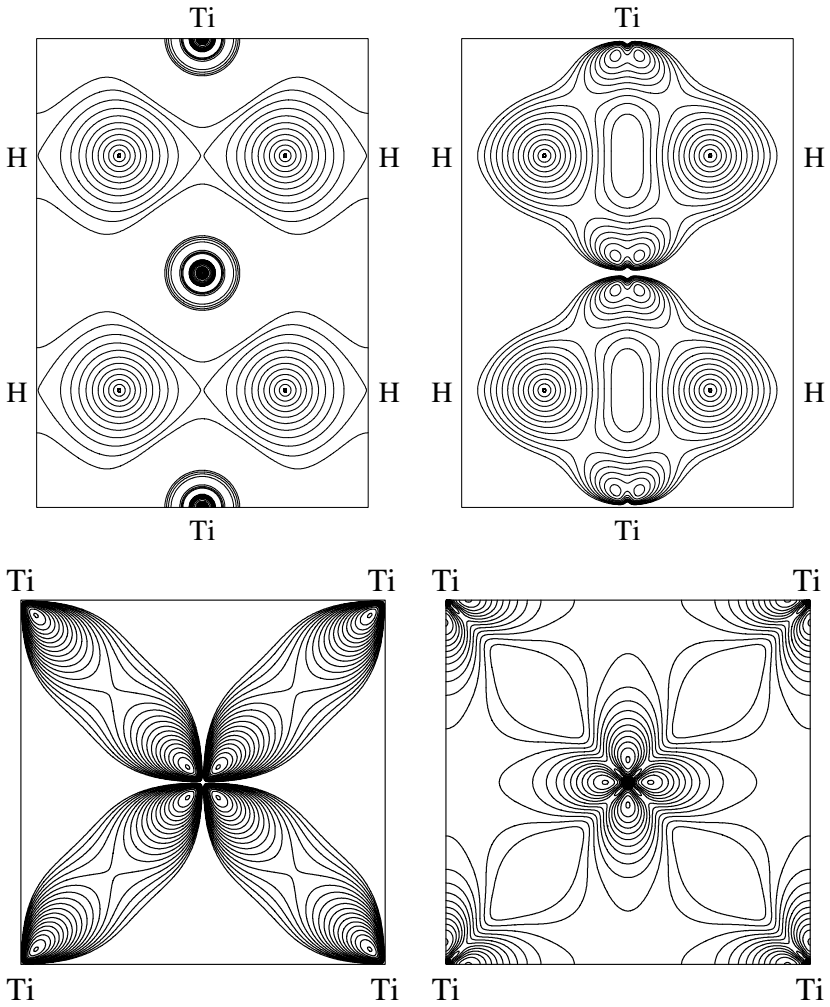

Figure 5. Electron densities for some characteristic states for fluorite-type TiH_2. Top left: the Γ state at -0.2606 Ryd in the (110) plane; top right: the X state at 0.0726 Ryd in the (110) plane; bottom left: the Γ state at 0.4855 Ryd in the (100) plane; bottom right: the X state at 0.2874 Ryd in the (100) plane. A logarithmic grid of contour lines has been used ($x_i = x_0 2^{i/3}$, $x_0 = 0.02\,e$ Å^{-3}).

zone corresponding to the Γ–N direction in the body-centred tetragonal Brillouin zone which is very close to the Fermi level. A similar situation is observed for the Γ–Δ and Γ–Σ directions. For the tetragonal structures this band is split into two bands such that in general one of the bands is below and one above the Fermi level and the band below the Fermi level for $c/a < 1$ is above the Fermi level for $c/a > 1$ and vice versa.

The DOS curves for tetragonally distorted TiH_2 and ZrH_2 are very similar to the corresponding DOS for the cubic compounds (figure 8). The most important differences are the changes in the close vicinity of the Fermi level caused by the splitting of bands in this region. As a consequence the Fermi level in the tetragonal case is not situated in a peak of the DOS but in a local minimum which leads to a reduced total energy. Good qualitative agreement with the LMTO-ASA results of Gupta (1998) and with the corrected DOS results of Ackland (1998b) is observed.

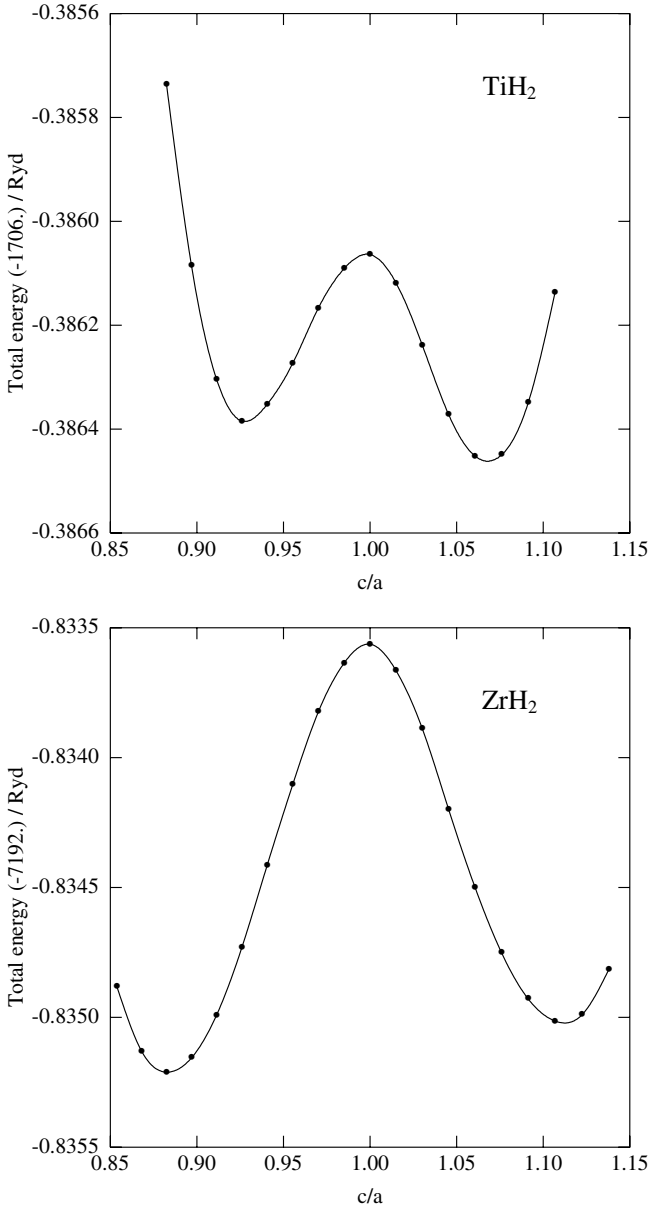

Figure 6. Total-energy curves for TiH_2 and ZrH_2 as functions of the c/a ratios. Please notice the different energy scales for the two compounds.

3.2.3. Electron densities and chemical bonding. In figure 9 the total valence electron densities for the tetragonal phases of TiH_2 are shown and compared to the densities for the occupied N state just below the Fermi level. It can be seen that the essential features of the valence electron density are determined by the occupied N state. For $c/a > 1$ the valence electron density in the (001) plane has slight t_{2g} character as found in the density for the N state which corresponds to t_{2g}–t_{2g} σ-bonding between the Ti atoms. The valence electron density in the (100) plane on the other hand is predominantly e_g-like as is the case for state N which corresponds to an

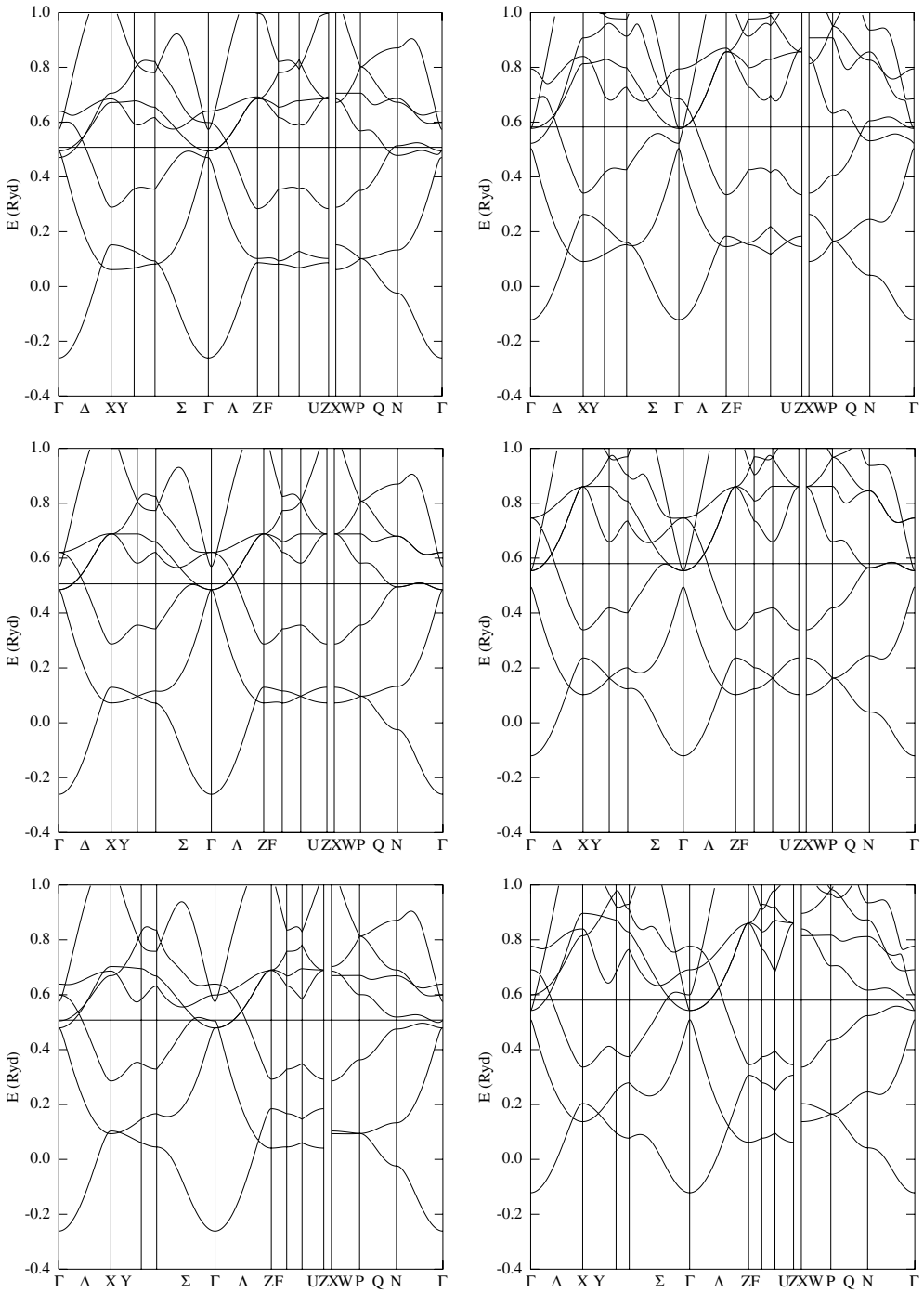

Figure 7. Band structures of TiH_2 (left column) and ZrH_2 (right column). Top row: for the tetragonally distorted fluorite structure with $c/a > 1$; central row: for the (cubic) fluorite structure plotted in the body-centred-tetragonal Brillouin zone; bottom row: for the tetragonally distorted fluorite structure with $c/a < 1$.

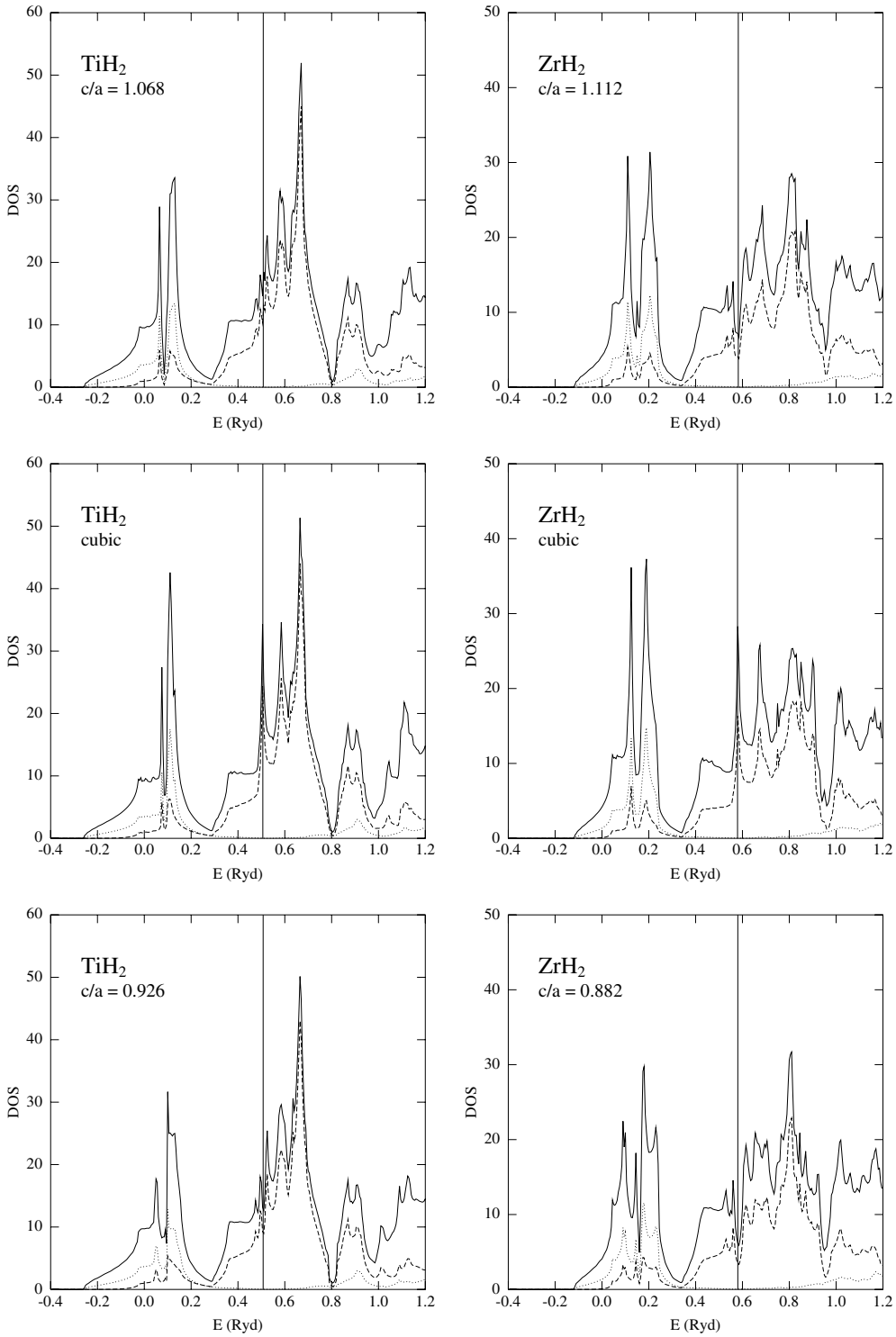

Figure 8. The total DOS (full line), and H s (dotted line) and transition metal d (dashed line) local partial DOS components for cubic and tetragonally distorted TiH_2 and ZrH_2 in units of one-electron states per Rydberg and per unit cell.

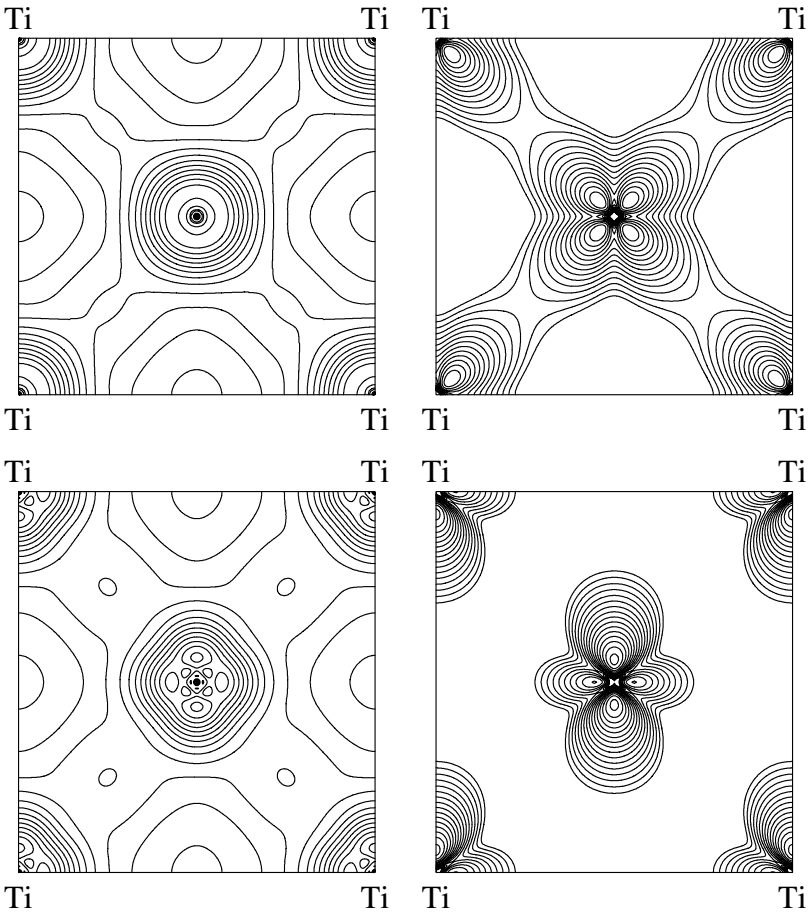

(a)

Figure 9. Comparison of valence electron densities (left) with electron densities for the N state (right) of tetragonally distorted TiH_2. (a) $c/a = 1.068$, N state at 0.478 Ryd; upper row: (001) plane; lower row: (100) plane; (b) $c/a = 0.926$, N state at 0.475 Ryd; upper row: (001) plane; lower row: (100) plane. A logarithmic grid of contour lines has been used ($x_i = x_0 2^{i/3}$, $x_0 = 0.2\ e$ Å^{-3} (left), $x_0 = 0.02\ e$ Å^{-3} (right)).

(antibonding) Ti–Ti e_g–e_g π^*-interaction. For $c/a < 1$ the situation is reversed as regards the (001) and (100) planes. For the N state above the Fermi level the density is e_g-like where it is t_{2g} for the corresponding N state below the Fermi level and vice versa, whereby the bonding character is slightly reduced compared to that of the occupied state.

4. Résumé

The present study provides a consistent description of fluorite-type dihydrides ScH_2, TiH_2, VH_2, YH_2, ZrH_2 and NbH_2 based on density functional theory. Lattice parameters and bulk moduli are derived from total-energy calculations and the electronic structure and chemical bonding is explored by means of band structures, DOS, local partial DOS and, for the first time, valence electron density plots.

Special attention is paid to TiH_2 and ZrH_2, for which a tetragonally distorted fluorite

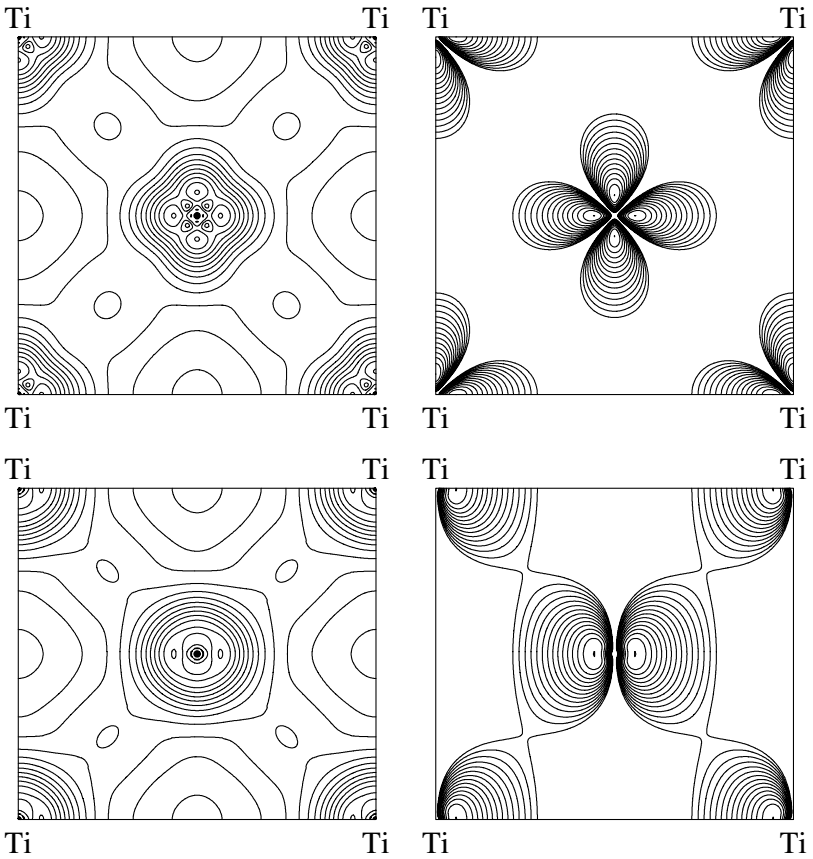

(b)

Figure 9. (Continued)

Table 4. Calculated equilibrium lattice parameters (this work) and experimental values (in Å) for the tetragonal dihydrides.

Compound		Calculated	Experimental	Remarks	References
TiH_2	a	4.513	4.528	$TiH_{1.99}$, 79 K	Yakel (1958)
	c	4.179	4.279		
	c/a	0.928	0.945		
	a	4.303			
	c	4.595			
	c/a	1.068			
ZrH_2	a	5.008	4.975	$ZrH_{2.0}$	Niedźwiedź *et al* (1993)
	c	4.419	4.447		
	c/a	0.883	0.894		
	a	4.635			
	c	5.157			
	c/a	1.113			

structure becomes stable at low temperatures. The structural transition is monitored with respect to total energies, band structures, DOS and electron densities. Consistent with the

experimental phase diagram, the fluorite structure is found to be unstable at 0 K. Tetragonal distortion leads to two almost equally stable structures with $c/a > 1$ and $c/a < 1$, the latter of which corresponds to the experimentally observed low-temperature phase. This tetragonal distortion is driven by a Jahn–Teller-type band split which opens up a pseudo-gap in the DOS at the Fermi level. The corresponding changes of the bond characteristics are discussed on the basis of electron densities.

Acknowledgments

The authors are grateful to Gerhard Schwarz and Alexander Pokorny for performing some of the calculations, to O J Żogał and P Vajda for helpful comments on the manuscript, and to the *Hochschuljubiläumsstiftung der Stadt Wien* (Project H-00095/96) for financial support of this work.

References

Ackland G J 1998a *Phys. Rev. Lett.* **80** 2233
Ackland G J 1998b *Phys. Rev. Lett.* **81** 3301
Birch F 1938 *J. Appl. Phys.* **9** 279
Birch F 1952 *J. Geophys. Res.* **57** 227
Birch F 1978 *J. Geophys. Res.* **83** 1257
Daou J N and Vajda P 1992 *Phys. Rev.* B **45** 10 907
Ducastelle F, Caudron R and Costa P 1970 *J. Physique* **31** 57
Elsässer C, Schweizer S and Fähnle M 1997 *Mater. Res. Soc. Symp. Proc.* **453** 221
Fujimori A and Tsuda N 1982 *Solid State Commun.* **41** 491
Fukai Y 1993 *The Metal–Hydrogen System. Basis Bulk Properties* (Berlin: Springer)
Gupta M 1979 *Solid State Commun.* **29** 47
Gupta M 1982 *Phys. Rev.* B **25** 1027
Gupta M 1998 *Phys. Rev. Lett.* **81** 3301
Gupta M and Schlapbach L 1988 *Hydrogen in Intermetallic Compounds I* ed L Schlapbach (Berlin: Springer) pp 139–217
Hedin L and Lundqvist B I 1971 *J. Phys. C: Solid State Phys.* **4** 2064
Hedin L and Lundqvist S 1972 *J. Physique Coll.* **33** C3 73
Herzig P, Wolf W and Żogał O J 1999 *Phys. Rev.* B submitted
Hjörvarsson B, Guo J-H, Ahuja R, Ward R C C, Andersson G, Eriksson O, Wells M R, Såthe C, Agui A, Butorin S M and Nordgren J 1999 *J. Phys.: Condens. Matter* **11** L119
Jansen H J F and Freeman A J 1984 *Phys. Rev.* B **30** 561
Jepsen O and Andersen O K 1971 *Solid State Commun.* **9** 1763
Kelly P J, Dekker J P and Stumpf R 1997 *Phys. Rev. Lett.* **78** 1315
Khodyrev Yu P and Baranova R V 1980 *Kristallografiya* **25** 172 (Engl. Transl. 1980 *Sov. Phys.–Crystallogr.* **25** 99)
Kulikov N I and Zvonkov A D 1979 *Z. Phys. Chem., NF* **117** 113
Lehmann G and Taut M 1972 *Phys. Status Solidi* b **54** 469
Matumura T, Yukawa H and Morinaga M 1999 *J. Alloys Compounds* **284** 82
Müller H and Weymann K 1986 *J. Less-Common Met.* **119** 115
Ng K K, Zhang F C, Anisimov V I and Rice T M 1997 *Phys. Rev. Lett.* **78** 1311
Niedźwiedź K, Nowak B and Żogał O J 1993 *J. Alloys Compounds* **194** 47
Nowak B and Minier M 1984 *J. Less-Common Met.* **101** 245
Nowak B, Żogał O J and Minier M 1979 *J. Phys. C: Solid State Phys.* **12** 4591
Nowak B, Żogał O J and Drulis H 1982 *J. Phys. C: Solid State Phys.* **15** 5829
Papaconstantopoulos D A, Laufer P M and Switendick A C 1986 *NATO ASI Series B* vol 136 (New York: Plenum) p 139
Papaconstantopoulos D A and Switendick A C 1984 *J. Less-Common Met.* **103** 317
Perdew J P and Wang Y 1992 *Phys. Rev.* B **45** 13 244
Peterman D J and Harmon B N 1979 *Phys. Rev.* B **20** 5313
Peterman D J, Harmon B N, Johnson D L and Marchiando J 1979a *Z. Phys. Chem., NF* **116** 47

Peterman D J, Harmon B N, Marchiando J and Weaver J H 1979b *Phys. Rev.* B **19** 4867
Reilly J J and Wiswall R H Jr 1970 *Inorg. Chem.* **9** 1678
Sen Gupta R and Chatterjee S 1982 *J. Phys. F: Met. Phys.* **12** 1923
Smith E 1995 *J. Mater. Sci.* **30** 5910
Sun S N, Wang Y and Chou M Y 1994 *Phys. Rev.* B **49** 6481
Switendick A C 1970 *Solid State Commun.* **8** 1463
Switendick A C 1976 *J. Less-Common Met.* **49** 283
Switendick A C 1984 *J. Less-Common Met.* **101** 191
Switendick A C 1987 *J. Less-Common Met.* **130** 249
Wang Y and Chou M Y 1994 *Phys. Rev.* B **49** 10 731
Wang Y and Chou M Y 1995 *Phys. Rev.* B **51** 7500
Wimmer E, Krakauer H, Weinert M and Freeman A J 1981 *Phys. Rev.* B **24** 864
Yakel H L Jr 1958 *Acta Crystallogr.* **11** 46
Żogał O J and Idziak S 1981 *Physica* B **104** 365
Żogał O J, Nowak B, Wolf W and Herzig P 1996 *Z. Phys.* B **101** 205
Żogał O J, Vuorimäki A H and Ylinen E E 1999 *Eur. Phys. J.* B **10** 201
Zuzek E, Abriata J P, San-Martin A and Manchester F D 1990 *Bull. Alloy Phase Diagrams* **11** 385